

Extended Multi-agent Consensus Protocols for the Generation of Geometric Patterns in the Plane

Panagiotis Tsiotras

Luis Ignacio Reyes Castro

Abstract—We propose a decentralized control law for multi-agent formations in two dimensions that allows the participating vehicles to display intricate periodic and quasi-periodic geometric patterns. Inspired by the “standard” consensus protocol $\dot{x} = -Lx$, these controls rely only on the relative position between the networked agents which are neighbors in the underlying communication graph. Several examples are presented, resulting in non-trivial geometric patterns described by trochoidal curves, similar to those generated by kids around the world using a spirograph. These paths can be useful for coordinated, distributed surveillance and monitoring applications, as well as for the sake of their own aesthetical beauty.

I. AN EXTENDED CONSENSUS PROTOCOL

Consensus problems have been extensively used in the past in the area of distributed computing and management science. Their recent popularity in the controls community stems from their utilization in formulating and solving a variety of multi-agent, mobile network problems [1], [2]. In this paper we propose a generalization of the standard consensus algorithm used widely in the literature [3], [4], [5], and we show how it can be utilized to generate intricate geometrical patterns for the ensuing agent paths. Using minimal assumptions, the proposed feedback control is able to generate geometric patterns for the agent trajectories that go beyond formation-type geometric models, which deal mainly with identical agents in cycle pursuit [6], [7], [8], [9].

Our inspiration comes from gyroscopic control strategies used in the wheeled robotics community [10] for obstacle avoidance. Since the proposed control law introduces circulation, it cannot be derived from a scalar potential, and hence it does not belong to the family of consensus control laws that are gradient-based. As an added benefit of the proposed extension, it is shown that this control law results in consensus points that lie outside the convex hull of the initial positions of the agents. This may be useful for obstacle avoidance and/or consensus with deception, for instance.

In the second part of the paper we particularize the proposed control law to the case of periodic and quasi-periodic pattern generation and show how it can be used to generate elaborate, aesthetically beautiful patterns, similar to those obtained using a spirograph.

P. Tsiotras is a Professor at the School of Aerospace Engineering, Georgia Institute of Technology, Atlanta, GA 30332-0150, USA, Email:tsiotras@gatech.edu

L. I. R. Castro is an undergraduate student at the School of Aerospace Engineering, Georgia Institute of Technology, Atlanta, GA 30332-0150, USA, Email:nacho_reyes@gatech.edu

II. MOTIVATING EXAMPLE

In order to demonstrate the main idea, we start with the simplest of cases, namely, two agents ($N = 2$) in the plane. The extension to the case of an arbitrary number of agents follows readily from this case and it is given in the next section, along with the stability analysis of the closed-loop system. To this end, assume a given global coordinate frame \mathcal{E} with origin O and two agents at locations \vec{r}_1 and \vec{r}_2 respectively. The kinematic equation for each agent is given by

$$\dot{\vec{r}}_i = \vec{u}_i, \quad i = 1, 2. \quad (1)$$

We assume that only the *relative* distance $\vec{r}_{12} = \vec{r}_1 - \vec{r}_2$ is known to agent no. 1 and, similarly, the relative distance $\vec{r}_{21} = -\vec{r}_{12}$ is available to agent no. 2. It can be easily shown [5] that the control law

$$\vec{u}_1 = -\gamma_1 \vec{r}_{12}, \quad \vec{u}_2 = -\gamma_2 \vec{r}_{21}, \quad \gamma_1 + \gamma_2 > 0 \quad (2)$$

achieves consensus. Furthermore, with this control law, the two agents will meet somewhere along the line segment initially connecting $\vec{r}_1(0)$ and $\vec{r}_2(0)$. Our first objective is to modify (2) in order to allow convergence of the agents to points that do not necessarily belong to the line segment (in general, the convex hull) defined by the initial position vectors.

The main observation here is that the control law (2) does not make use of all available geometric information to each agent. For instance, agent no. 1 knows not only the vector \vec{r}_{12} but also all vectors (directions) *perpendicular* to \vec{r}_{12} , which can then be used in a feedback strategy. Similarly for agent no. 2. This additional information in the control law, inferred from—but distinct than—the relative position vector between the agents, can lead to more flexibility for trajectory design. To this end, let \vec{q}_{12} and \vec{q}_{21} be such that $\vec{q}_{12} \cdot \vec{r}_{12} = \vec{q}_{21} \cdot \vec{r}_{21} = 0$, and assume the following control laws¹

$$\vec{u}_1 = -\gamma_1 \vec{r}_{12} + \beta_1 \vec{q}_{12}, \quad \vec{u}_2 = -\gamma_2 \vec{r}_{21} + \beta_2 \vec{q}_{21} \quad (3)$$

Later it is shown that this control law also achieves consensus for $\gamma_1 + \gamma_2 > 0$ and $\beta_1, \beta_2 \in \mathbb{R}$.

In preparation for the general case, let us now introduce coordinates, with respect to a global frame \mathcal{E} , leading to $[\vec{r}_i]_{\mathcal{E}} \triangleq x_i \in \mathbb{R}^2$, ($i = 1, 2$) and $[\vec{r}_{12}]_{\mathcal{E}} = [\vec{r}_1]_{\mathcal{E}} - [\vec{r}_2]_{\mathcal{E}} = x_1 - x_2$. Let the error vector $z \in \mathbb{R}^2$ of the relative distance between the two agents be

$$z \triangleq x_1 - x_2 = d_{11}x_1 + d_{21}x_2 = (D^T \otimes I_2)x, \quad (4)$$

¹Owing to the freedom in choosing \vec{q}_{12} and \vec{q}_{21} , we define a “position orientation” such that $\vec{r}_{12} \times \vec{q}_{12} = \vec{r}_{21} \times \vec{q}_{21}$.

where $D = \begin{bmatrix} 1 & -1 \end{bmatrix}^\top$ and where $x = [x_1^\top, x_2^\top]^\top \in \mathbb{R}^4$. Furthermore, let $[\tilde{q}_{12}]_{\mathcal{E}} \stackrel{\Delta}{=} p = Sz$ where S is the skew symmetric matrix

$$S = \begin{bmatrix} 0 & -1 \\ 1 & 0 \end{bmatrix}. \quad (5)$$

It is clear that $p^\top z = z^\top p = 0$. It can then be easily seen that the control law (3) can be written compactly, as follows

$$\begin{aligned} u &= -(\Gamma \otimes I_2)(D \otimes I_2)z + (B \otimes I_2)(D \otimes I_2)Sz \\ &= -(\Gamma D \otimes I_2)z + (BD \otimes S)z, \end{aligned} \quad (6)$$

where $u = [u_1^\top, u_2^\top]^\top \in \mathbb{R}^4$ and $\Gamma = \text{diag}(\gamma_1, \gamma_2)$ and $B = \text{diag}(\beta_1, \beta_2)$. From (4) it follows that the error equation is given by

$$\begin{aligned} \dot{z} &= (D^\top \otimes I_2)\dot{x} = (D^\top \otimes I_2)u \\ &= -(D^\top \otimes I_2)(\Gamma \otimes I_2)(D \otimes I_2)z + (D^\top \otimes I_2)(B \otimes I_2)(D \otimes I_2)Sz \\ &= -((D^\top \Gamma D) \otimes I_2)z + ((D^\top B D) \otimes S)z. \end{aligned}$$

Stability is determined by the eigenvalues of the matrix $A_{\text{CL}} = -((D^\top \Gamma D) \otimes I_2) + ((D^\top B D) \otimes S)$. A simple calculation shows that $\text{spec}(A_{\text{CL}}) = \{-(\gamma_1 + \gamma_2) \pm i(\beta_1 + \beta_2)\}$. Hence consensus is achieved asymptotically as long as $\gamma_1 + \gamma_2 > 0$. The ‘‘classical’’ consensus control law (2) corresponds to the case when $\beta_1 = \beta_2 = 0$. When $B \neq 0$ stability is still maintained, however, the transient response is different. Furthermore, the point where consensus is achieved can be selected to lie outside the line segment connecting $x_1(0)$ and $x_2(0)$ by a proper choice of the gains β_1 and β_2 . This is demonstrated in Fig. 1 where the result of a simulation with the data $x_1(0) = (-1, 1)^\top, x_2(0) = (2, 3)^\top, \Gamma = \text{diag}(0.1, 1), B = \text{diag}(-0.5, 2)$ is shown. For this example the two agents meet at the point with coordinates $(-2, 1)$.

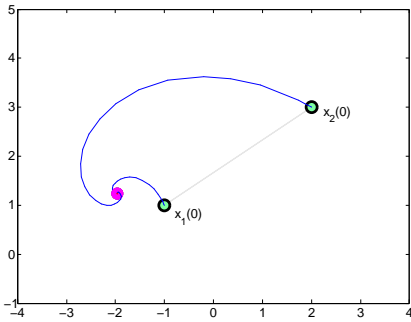


Fig. 1. Numerical example with ‘‘skew-symmetric’’ feedback. The skew-symmetric term creates a vector field with circulation.

III. EXTENSION TO N AGENTS IN THE PLANE

For the general case, consider N agents in the plane. Assume that their location is given by the state variables $x_i \in \mathbb{R}^2$ for $i = 1, \dots, N$, expressed in the same, common global frame \mathcal{E} , satisfying the differential equations

$$\dot{x}_i = u_i, \quad i = 1, \dots, N. \quad (7)$$

To the N agents we associate a graph \mathcal{G} that describes the communication topology between the agents. That is, \mathcal{G} has N nodes and M edges (links), with each edge denoting knowledge of the relative position between the corresponding agents. We can define the incidence matrix $D \in \mathbb{R}^{N \times M}$ with elements as follows [11]. We assign $d_{ij} = +1$ (-1) if the i th node is the head (tail) of j th edge, and $d_{ij} = 0$ otherwise. If the i th agent is a neighbor with the j th agent, then they are connected by an edge, and we have the difference (error) variable

$$z_k = \sum_{\ell=1}^N d_{\ell k} x_\ell = \begin{cases} x_i - x_j, & \text{if } i \text{ is the head,} \\ x_j - x_i, & \text{if } j \text{ is the head,} \end{cases} \quad (8)$$

where $z_k \in \mathbb{R}^2$ for $k = 1, \dots, M$. If the columns of D are linearly independent, that is, if the graph does not contain cycles, then the vectors z_k are linearly independent [11]. Note also that the graph is connected if and only if $\text{rank} D = N - 1$ [3], [12]. Introducing the stack vector $x = [x_1^\top \ \dots \ x_N^\top]^\top \in \mathbb{R}^{2N}$, the state equations (7) can be written compactly as

$$\dot{x} = u, \quad (9)$$

where $u = [u_1^\top \ \dots \ u_N^\top]^\top \in \mathbb{R}^{2N}$. Following (6), we propose the control law

$$u = -(\Gamma D \otimes I_2)z + (BD \otimes S)z, \quad (10)$$

where $z = [z_1^\top \ \dots \ z_M^\top]^\top \in \mathbb{R}^{2M}$, and where $\Gamma = \text{diag}(\gamma_1, \dots, \gamma_N)$ and $B = \text{diag}(\beta_1, \dots, \beta_N)$. The standard consensus algorithm results as a special case of (10) where $B = 0$.

Convergence Analysis

From (8) it can be easily shown that the error vector z can be written compactly as follows

$$z = (D^\top \otimes I_2)x. \quad (11)$$

From (10) the differential equation for x is then given by

$$\begin{aligned} \dot{x} &= -(\Gamma D \otimes I_2)(D^\top \otimes I_2)x + (BD \otimes S)(D^\top \otimes I_2)x \\ &= -((\Gamma D D^\top) \otimes I_2 - (B D D^\top) \otimes S)x \\ &= -((\Gamma L) \otimes I_2 - (B L) \otimes S)x, \end{aligned} \quad (12)$$

where $L \stackrel{\Delta}{=} D D^\top \in \mathbb{R}^{N \times N}$ is the *graph Laplacian* [5]. Let $\mathbf{1}_N \stackrel{\Delta}{=} (1, 1, \dots, 1)^\top \in \mathbb{R}^N$ denote the N -dimensional column vector of ones, and recall that $L \mathbf{1}_N = 0$ [5], [12]. For any $v \in \mathbb{R}^2$ we have that $((\Gamma L) \otimes I_2 - (B L) \otimes S)(\mathbf{1}_N \otimes v) = (\Gamma L \mathbf{1}_N) \otimes v - (B L \mathbf{1}_N) \otimes (Sv) = 0$. It follows that the vector $\mathbf{1}_N \otimes v$ spans the null space of the matrix in (12). The equilibrium point \bar{x}_∞ of the linear differential equation (12) therefore satisfies the condition $\bar{x}_\infty \stackrel{\Delta}{=} \lim_{t \rightarrow \infty} x(t) = \mathbf{1}_N \otimes x_\infty$ for some $x_\infty \in \mathbb{R}^2$, from which it follows that $\lim_{t \rightarrow \infty} x_1(t) = \lim_{t \rightarrow \infty} x_2(t) = \dots = \lim_{t \rightarrow \infty} x_N(t) = x_\infty$, thus achieving consensus.

Let the coordinates of the final consensus point be $x_\infty = [x_\infty \ y_\infty]^\top \in \mathbb{R}^2$. We have the following proposition.

Proposition 1 ([13]): Let $v_1, v_2 \in \mathbb{R}^{2N}$ be such that $\text{span}\{v_1, v_2\} = \mathcal{R}^\perp((\Gamma L) \otimes I_2 - (B L) \otimes S)$. The final rendezvous point is given by

$$x_\infty = \begin{bmatrix} x_\infty \\ y_\infty \end{bmatrix} = \begin{bmatrix} v_1^\top (\mathbf{1}_N \otimes I_2) \\ v_2^\top (\mathbf{1}_N \otimes I_2) \end{bmatrix}^{-1} \begin{bmatrix} v_1^\top x(0) \\ v_2^\top x(0) \end{bmatrix}. \quad (13)$$

IV. PERIODIC AND QUASI-PERIODIC TRAJECTORIES

Given an interconnection topology, the particular choices of the gain matrices Γ and B can be used to generate specific trajectory patterns for the agent paths. Since we are mainly interested in periodic or quasi-periodic trajectories, next we restrict the discussion to the case $\Gamma = 0$. By letting $\Gamma = 0$ in (12) the closed-loop system reduces to

$$\dot{x} = ((BL) \otimes S)x. \quad (14)$$

The shape and frequencies of the resulting paths/trajectories are therefore determined by the eigenvalues and eigenvectors of the matrix $(BL) \otimes S$. Recall from the properties of the Kronecker product that the eigenvalues of the matrix $(BL) \otimes S$ are of the form $\lambda\mu$ where $\lambda \in \text{spec}(BL)$ and $\mu \in \text{spec}S$. Additionally, the corresponding eigenvectors are of the form $v \otimes u$ where $v \in \mathbb{C}^3$ is the eigenvector of the matrix BL associated with λ and $u \in \mathbb{C}^2$ is the eigenvector of the matrix S associated with μ . Since $\det(\lambda I_N - BL) = \det(\lambda I_N - BDD^T) = \det(\lambda I_M - D^TBD)$ it follows that the nonzero eigenvalues of the matrix BL coincide with the nonzero eigenvalues of D^TBD . Because the latter matrix is symmetric, all eigenvalues of BL are real. Consequently, all eigenvalues of $(BL) \otimes S$ lie on the imaginary axis. It follows that the solutions of (14) consist, in general, of a superposition of sine and cosine functions, perhaps multiplied by polynomials in t (in the case of multiple eigenvalues).

Let $BL = VJV^{-1}$ be the spectral decomposition of the matrix BL . It can be easily shown that

$$e^{((BL) \otimes S)t} = (V \otimes I_2) e^{(J \otimes S)t} (V^{-1} \otimes I_2). \quad (15)$$

The spectral decomposition of the matrix BL thus provides all information needed to investigate the nature of the solutions of (14). In fact, additional information can be gathered owing to the special structure of the state matrix in (14).

Lemma 1: Let A be an $n \times n$ square matrix and let S be the 2×2 skew symmetric matrix given in (5). Then

$$e^{A \otimes S} = \cos A \otimes I_2 + \sin A \otimes S. \quad (16)$$

Proof: Notice that $S^{2k} = (-1)^k I_2$ and $S^{2k+1} = (-1)^k S$, $k = 0, 1, 2, \dots$ and recall that

$$e^{A \otimes S} = \sum_{k=0}^{\infty} \frac{1}{k!} (A \otimes S)^k.$$

The rhs of the previous equation can be expanded as follows

$$\begin{aligned} & \sum_{k=0}^{\infty} \frac{1}{(2k)!} (A \otimes S)^{2k} + \sum_{k=0}^{\infty} \frac{1}{(2k+1)!} (A \otimes S)^{2k+1} \\ &= \sum_{k=0}^{\infty} \frac{1}{(2k)!} (A^{2k} \otimes S^{2k}) + \sum_{k=0}^{\infty} \frac{1}{(2k+1)!} (A^{2k+1} \otimes S^{2k+1}) \\ &= \left(\sum_{k=0}^{\infty} \frac{(-1)^k}{(2k)!} A^{2k} \right) \otimes I_2 + \left(\sum_{k=0}^{\infty} \frac{(-1)^k}{(2k+1)!} A^{2k+1} \right) \otimes S. \end{aligned}$$

Making use of the fact that for a square matrix A ,

$$\cos A = \sum_{k=0}^{\infty} \frac{(-1)^k}{(2k)!} A^{2k}, \quad \sin A = \sum_{k=0}^{\infty} \frac{(-1)^k}{(2k+1)!} A^{2k+1},$$

the result of the lemma follows immediately. \blacksquare

We therefore have the following Proposition.

Proposition 2: The solution of (14) is given by

$$\begin{aligned} x(t) &= (\cos(BLt) \otimes I_2 + \sin(BLt) \otimes S)x(0), \\ &= (V \otimes I_2) (\cos(Jt) \otimes I_2 + \sin(Jt) \otimes S) (V^{-1} \otimes I_2) x(0), \end{aligned} \quad (17)$$

for all $t \geq 0$ and all $x(0) \in \mathbb{R}^{2N}$.

The structure of the state matrix in (14) (e.g., its eigenvalues and eigenvectors) thus can provide a great deal of information regarding the paths followed by the agents in the Cartesian coordinate frame, as well as the relative location of the agents on these paths (i.e., their relative phasing). For instance, one can ensure that the agent trajectories either form closed paths with given phasing, or they form a dense set of trajectories, ensuring that almost every point in a given region will be visited at least once by one or more agents.

V. ORBIT PATTERN GENERATION

A. A Family of Achievable Paths

The solutions in (17) fall in the general class of *trochoidal* curves, which includes ellipses (and circles), epitrochoids, hypotrochoids, as well as cardioids, astroids, limaçons, and all polar coordinate roses [14]. An *epitrochoid* curve is generated by a point P attached at a radial distance d from the center of a circle of radius r , which is rolling without slipping around a circular track of radius R . The distance d can be smaller, equal, or greater than the radius r of the rolling circle. The ratio of the circular two tracks $k = R/r$ indicates the number of points at which the agent is closest to the center of the circular track. These are referred to as *crests*. In the special case when $r = d$, the curve becomes an *epicycloid* with k cusps; at these points, the curve is not differentiable. Note that ellipsoidal paths correspond to the case when $k = 0$. A *hypotrochoid* is generated by a point P attached at a distance d from the center of a circle of radius r , which rolls inside a circle of radius R . Again, the distance d can be smaller, equal, or greater than the radius r of the rolling circle; this radius, however, cannot exceed that of the circle R .

B. Illustrative Example: Three Agents

In this section we investigate in greater detail the simple non-trivial case, namely, three agents in the plane ($N = 3$), connected either in a path graph ($M = 2$) or a complete graph ($M = 3$). For a path graph interconnection the incidence matrix is given by

$$D = \begin{bmatrix} -1 & 0 \\ 1 & -1 \\ 0 & 1 \end{bmatrix}. \quad (18)$$

A straightforward calculation shows that the two nonzero eigenvalues of the matrix BL for this case are given by

$$\frac{\beta_1}{2} + \beta_2 + \frac{\beta_3}{2} \pm \frac{\sqrt{\beta_1^2 - 2\beta_1\beta_3 + 4\beta_2^2 + \beta_3^2}}{2}.$$

For the complete graph the incidence matrix is given by

$$D = \begin{bmatrix} -1 & 0 & 1 \\ 1 & -1 & 0 \\ 0 & 1 & -1 \end{bmatrix}. \quad (19)$$

The nonzero eigenvalues of the matrix BL for this case are given by

$$\beta_1 + \beta_2 + \beta_3 \pm \sqrt{\beta_1^2 + \beta_2^2 + \beta_3^2 - \beta_1\beta_2 - \beta_2\beta_3 - \beta_3\beta_1}.$$

The ratio of the two nonzero eigenvalues is equal to $k+1$ for an epitrochoid or $k-1$ for a hypotrochoid. Note that if k turns out to be an irrational number, then the number of crests is infinite, which means that the curve does not close; instead, the trajectories form a dense subset of the space [15]. An orbit redesign can yield periodic orbits of a particular shape that can be used for coordinated, distributed surveillance and perimeter monitoring applications; see, for instance, Fig. 2. Such an orbit redesign will require however, in general, a complete interconnection topology [13].

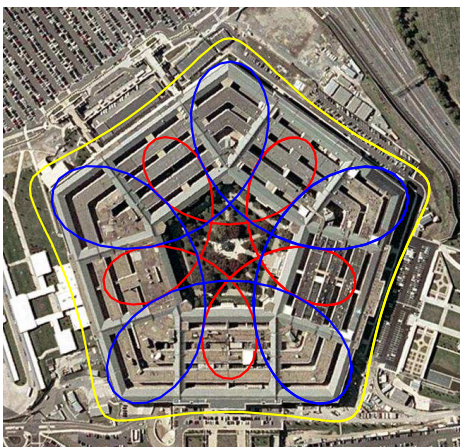


Fig. 2. Three agents patrolling a pentagon.

An interesting case occurs when the closed loop system has two zero eigenvalues at the origin. In this case the trajectories exhibit secular motion. Figure 3(a) shows the trajectories when $B = \text{diag}(0.5, -1, -1)$. It can be easily verified that in this case the relative orbits for the three agents are all circles; see Fig. 3(b).

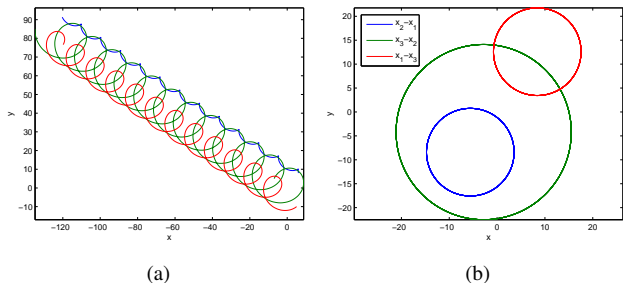


Fig. 3. $B = \text{diag}(0.5, -1, -1)$ and initial conditions $x_1(0) = (6, 8)$, $x_2(0) = (-7, 5)$, $x_3(0) = (5, -10)$ (path graph interconnection). The figure on the right shows the relative orbits.

VI. A GALLERY OF ORBITS

Clearly, one can generate a myriad of beautiful geometric patterns by changing the gain matrix B and by choosing a

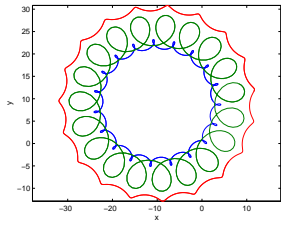
suitable graph Laplacian L in (14). Figures 4-7 provide a glimpse on the plethora and variety of geometric patterns generated using the consensus control law in (14) for the case of three and four agents. We urge the reader to try his/her own skills at generating visually pleasing curves using (14).

VII. CONCLUSIONS

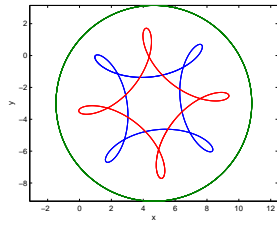
We have presented an extension of the classical consensus algorithm for multi-agent systems to achieve consensus outside the convex hull of the initial conditions of the agents. As a by-product of this idea, we have shown how to generate agent trajectories leading to intricate geometric patterns in the plane using only relative, local information. Future work will concentrate on developing a general theory for orbit design for an arbitrary number of agents in two, and three dimensions. Apart from their inherent aesthetical appeal, these orbits can have immediate applications in the area of coordinated, persistent surveillance and monitoring using a team of agents interacting using local information.

REFERENCES

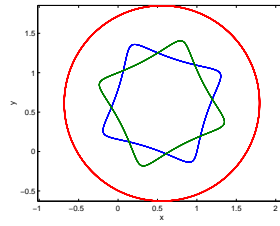
- [1] R. Olfati-Saber, J. A. Fax, and R. M. Murray, "Consensus and cooperation in multi-agent networked systems," *Proceedings of the IEEE*, vol. 97, pp. 215–233, 2006.
- [2] W. Ren and R. W. Beard, "Consensus seeking in multi-agent systems using dynamically changing interaction topologies," *IEEE Trans. on Automatic Control*, vol. 50, no. 5, pp. 655–661, 2005.
- [3] R. Olfati-Saber and R. M. Murray, "Consensus problems in networks of agents with switching topology and time-delays," *IEEE Trans. on Automatic Control*, vol. 49, no. 9, pp. 1520–1533, 2004.
- [4] J. A. Fax and R. M. Murray, "Information flow and cooperative control of vehicle formations," *IEEE Transactions on Automatic Control*, vol. 49, no. 9, pp. 1465–1476, 2004.
- [5] M. Mesbahi and M. Egerstedt, *Graph Theoretic Methods in Multiagent Networks*. Princeton, New Jersey: Princeton University Press, 2010.
- [6] I. Suzuki and M. Yamashita, "Distributed anonymous mobile robots: Formation of geometric patterns," *SIAM J. on Computing*, vol. 28, no. 4, pp. 1347–1363, 1999.
- [7] M. Pavone and E. Frazzoli, "Decentralized policies for geometric pattern formation and path coverage," *Journal of Dynamic Systems, Measurement, and Control*, vol. 129, pp. 633–643, 2007.
- [8] N. E. Leonard and E. Fiorelli, "Virtual leaders, artificial potentials, and coordinated control of groups," *Proc. of the 40th IEEE Conference on Decision and Control*, pp. 2968–2973, 2001.
- [9] J. A. Marshall, M. E. Broucke, and B. A. Francis, "Formations of vehicles in cyclic pursuit," *IEEE Trans. on Automatic Control*, vol. 49, no. 11, pp. 1963–1974, 2004.
- [10] L.-S. Wang and P. S. Krishnaprasad, "Gyroscopic control and stabilization," *Journal of Nonlinear Science*, vol. 2, pp. 367–415, 1992.
- [11] M. Arcak, "Passivity as a design tool for group coordination," *IEEE Transactions on Automatic Control*, vol. 52, no. 8, pp. 1380–1390, 2007.
- [12] C. Godsil and G. Royle, *Algebraic Graph Theory*. Springer New York, 2001.
- [13] P. Tsiotras and L. I. Reyes Castro, "A note on the consensus protocol with some applications to agent orbit pattern generation," in *10th Symposium on Distributed Autonomous Robotic Systems (DARS)*, (Lausanne, Switzerland), Nov. 1–3, 2010.
- [14] L. Hall, "Trochoids, Roses, and Thorns—Beyond the Spirograph," *College Mathematics Journal*, vol. 23, no. 1, pp. 20–35, 1992.
- [15] J. Lawrence, *A Catalog of Special Plane Curves*. Dover Publications, first ed., June 1972.



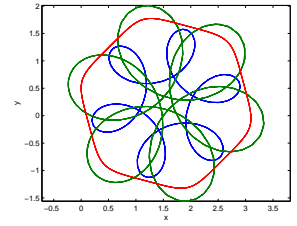
(a) $B = \text{diag}(1, 2.0034, -1)$.



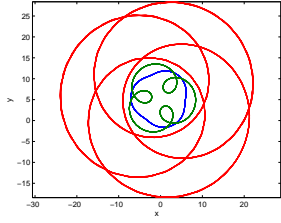
(b) $B = \text{diag}(-1, 2, -1)$.



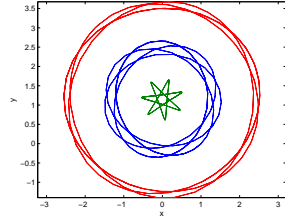
(a) $B = \text{diag}(1, 1, -5)$.



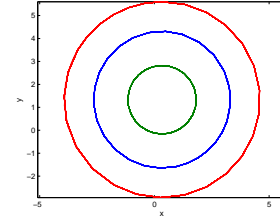
(b) $B = \text{diag}(1, 1.5492, -1)$.



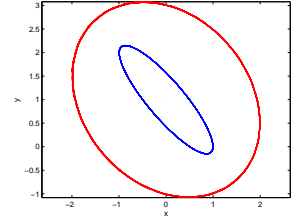
(c) $B = \text{diag}(1, 1, 6.0451)$.



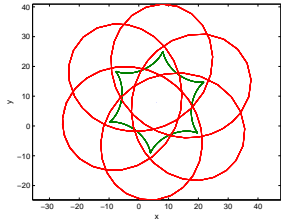
(d) $B = \text{diag}(-1, -0.1443, 1)$.



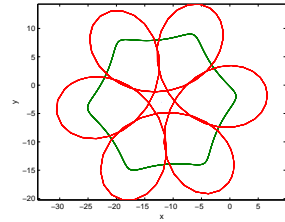
(c) $B = \text{diag}(1, 1, 1)$.



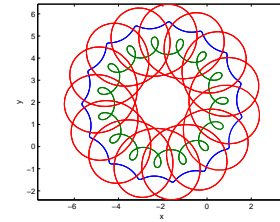
(d) $B = \text{diag}(-1, 0, 1)$.



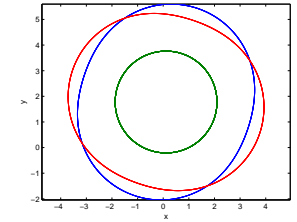
(e) $B = \text{diag}(0, 1, -6.5933)$.



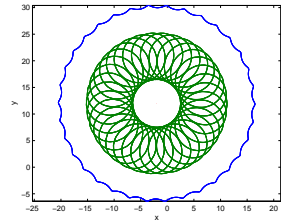
(f) $B = \text{diag}(0, 1, -6.5933)$.



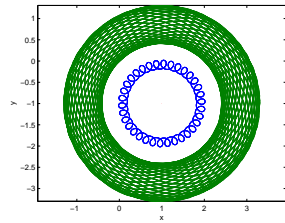
(e) $B = \text{diag}(-1, 1, 3)$.



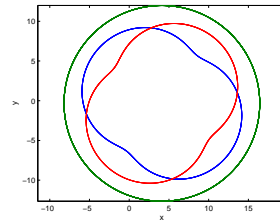
(f) $B = \text{diag}(0.5, 2, 0.5)$.



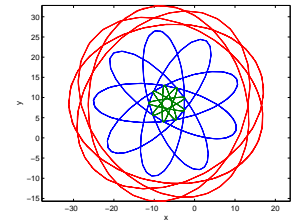
(g) $B = \text{diag}(1, -8.7289, 0)$.



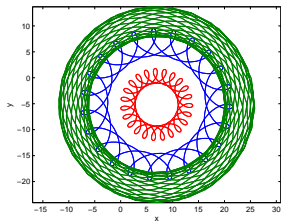
(h) $B = \text{diag}(1, -8.7289, 0)$.



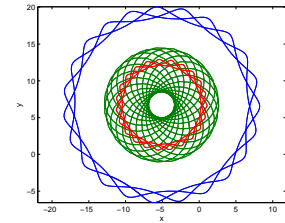
(g) $B = \text{diag}(0.5, 2, 0.5)$.



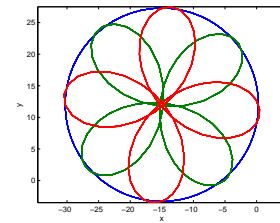
(h) $B = \text{diag}(-1, -0.1936, 1)$.



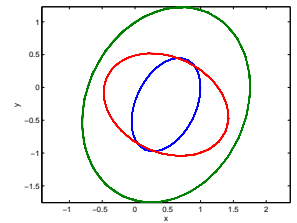
(i) $B = \text{diag}(1, -2.9054, 0.5)$.



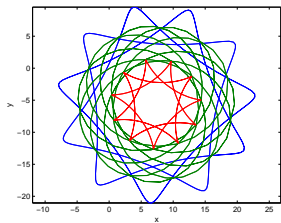
(j) $B = \text{diag}(1, -2.9054, 0.5)$.



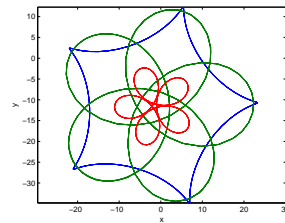
(i) $B = \text{diag}(4, -4, -4)$.



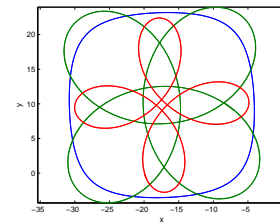
(j) $B = \text{diag}(-5, 3, 2)$.



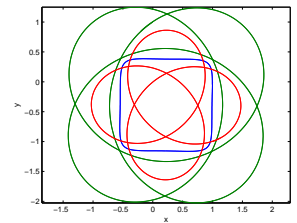
(k) $B = \text{diag}(1, -1.3935, 0.5)$.



(l) $B = \text{diag}(1 - 1 - 0.5)$.



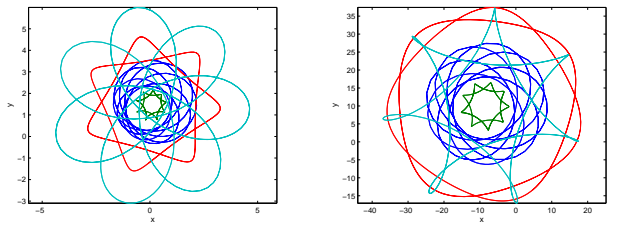
(k) $B = \text{diag}(-2.4736, 3, 2)$.



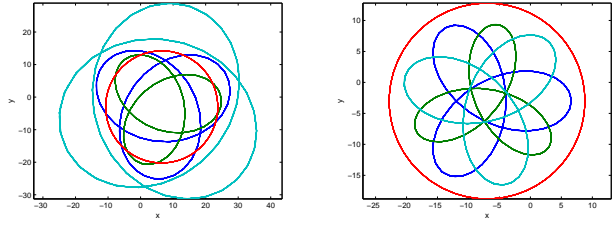
(l) $B = \text{diag}(-2.4736, 3, 2)$.

Fig. 4. A menagerie of orbits with three agents using the extended consensus protocol; path graph.

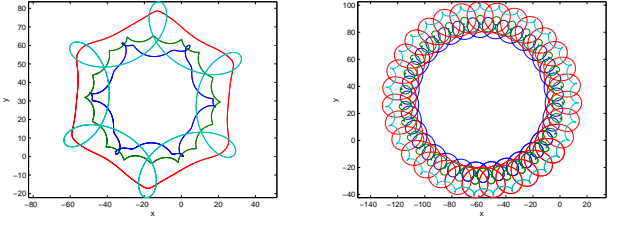
Fig. 5. A menagerie of orbits with three agents using the extended consensus protocol; complete graph.



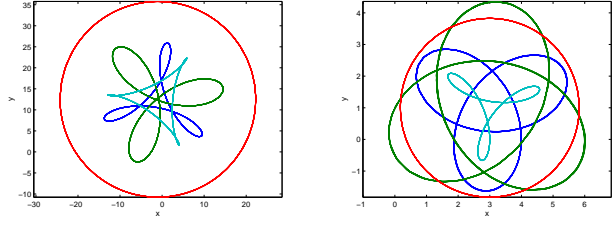
(a) $B = \text{diag}(2, 0.1826, -0.6126, 2)$. (b) $B = \text{diag}(2, 0.1826, -0.6126, 2)$.



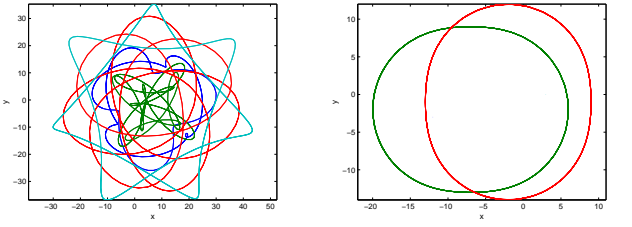
(a) $B = \text{diag}(-1, -1, +1, -1)$. (b) $B = \text{diag}(-1, -1, +1, -1)$.



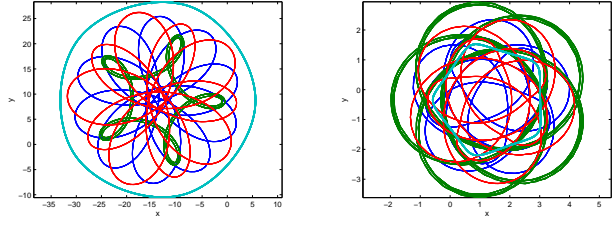
(c) $B = \text{diag}(2, 1.7141, -0.8257, 2)$. (d) $B = \text{diag}(2, 3.622, 2.336, -1)$.



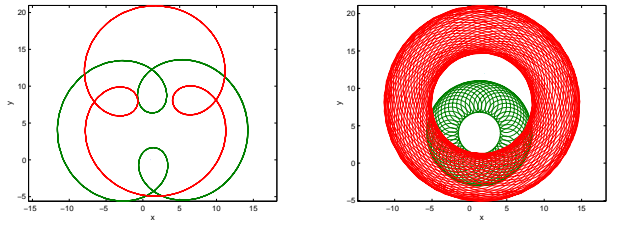
(c) $B = \text{diag}(-1, -1, +1, -1)$. (d) $B = \text{diag}(-1, -1, +1, -1)$.



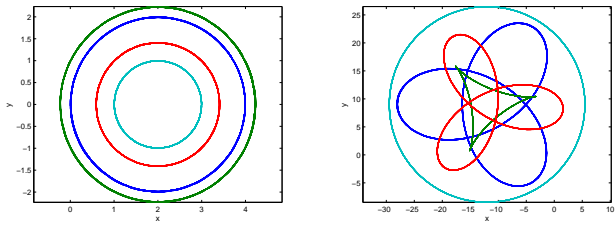
(e) $B = \text{diag}(-1, -1.145, 1.297, -1)$. (f) $B = \text{diag}(0, -1, -1, 0)$.



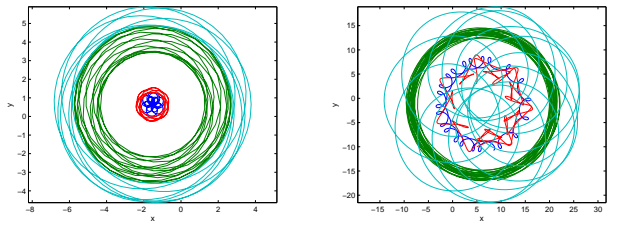
(e) $B = \text{diag}(-2, -4.133, -2.074, +2)$. (f) $B = \text{diag}(-2, -4.133, -2.074, +2)$.



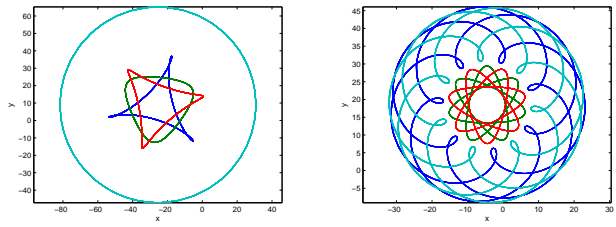
(g) $B = \text{diag}(0, -1, -1, 0)$. (h) $B = \text{diag}(0, -1, -3, 0)$.



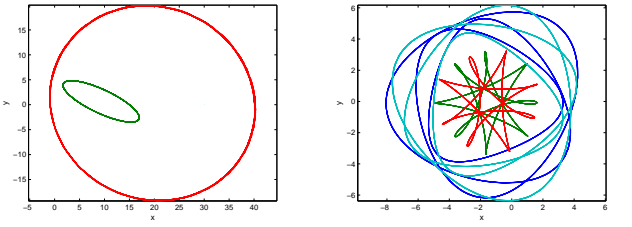
(g) $B = \text{diag}(-2, -2, -2, -2)$. (h) $B = \text{diag}(-2, -2, -2, 2)$.



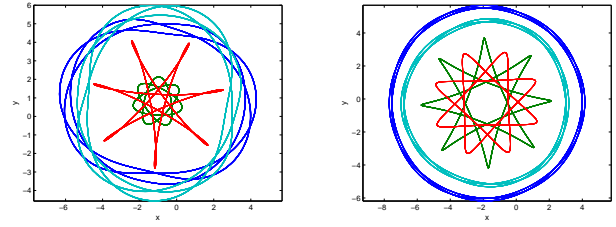
(i) $B = \text{diag}(0.15, -1, 0.15, -1)$. (j) $B = \text{diag}(0.15, -1, 0.15, 1)$.



(i) $B = \text{diag}(-2, -2, -2, 2)$. (j) $B = \text{diag}(5, -2, -2, 5)$.



(k) $B = \text{diag}(0, -1, 1, 0)$. (l) $B = \text{diag}(5, -2, -2, 5)$.



(k) $B = \text{diag}(5, -0.866, -3.208, 5)$. (l) $B = \text{diag}(3.229, -2, -1.515, 5)$.

Fig. 6. Sample orbits with four agents using the extended consensus protocol; path graph.

Fig. 7. Sample orbits with four agents using the extended consensus protocol; complete graph.